(Online) ISSN 2712-0562
Sustainable Engineering and Innovation *Original Research*
Vol. 7, No. 1, 2025, pp.147-158
https://doi.org/10.37868/sei.v7i1.id472

New microstrip bandpass filter design with sharp roll-off based on rectangular split resonators

Aqeel H. Al-Fatlawi[1,2], Sadra Kashef [3*], Yaqeen Sabah Mezaal[4,5], Morteza Valizadeh[6]
[1,3,6] Department of Electrical and Computer Engineering, Urmia University, Urmia, Iran
[2] Department of Computer Techniques Engineering, Imam Al-Kadhim University College (IKC), Iraq
[4] University of Information Technology and Communications, Baghdad, Iraq
[5] Al-Farahidi University, Baghdad, Iraq

*Corresponding author E-mail: s.kashef@urmia.ac.ir

Received Feb. 12, 2025
Revised Apr. 10, 2025
Accepted Apr. 16, 2025
Online Apr. 30, 2025

Abstract

This paper presents a compact bandpass filter (BPF) with a triple rectangular split resonator optimized for high performance at a central frequency of 3.682 GHz. The filter achieves an exceptional voltage standing wave ratio (VSWR) of 1.088 and a return loss of 27.48 dB, demonstrating superior impedance matching. Additionally, the filter exhibits minimal insertion loss with S21=0.38dB, ensuring efficient signal transmission. The design boasts a sharp roll-off rate of 87 and a narrow transition band of 0.196 GHz, making it suitable for high-selectivity applications. The compact size of the filter, measuring only 24 mm×24 mm, enhances its applicability in modern communication systems with limited space requirements.

Keywords: Microstrip resonators, Bandpass filter, Microwave filters, VSWR

1. Introduction

Filters are crucial components of many RF and microwave systems, used for both the separation and combination of frequencies. Since the electromagnetic spectrum is finite and public, RF/microwave signals are constrained to spectral bounds using filters. For example, the drive towards complete wireless communication pushes demand for these filters to exhibit improved performance while becoming smaller in size and mass, and less expensive. Based on the underlying technology used for their design and implementation, RF and microwave filters can be classified into two major categories: active and passive, according to specific requirements and technical specifications [1].

Active filters use active components such as transistors, diodes, amplifiers, and passive elements. These are relatively easy to implement and provide a gain with a high-quality factor attainable. They also combine effortlessly with the rest of the system components. However, the need for active components implies at least a power supply externally supplied, which may complicate the overall system's complexity [2]. Passive filters are constructed using passive components like capacitors and inductors. These filters offer several advantages over active filters, such as increased stability, no need for a power supply, and lower cost. In the microwave frequency range, particularly above 500 MHz, passive filters are typically implemented using planar transmission lines or

waveguides. While waveguide components have the benefits of low losses and the ability to handle higher power, they are less favored in modern communication systems that prioritize mobility due to their larger size and heavier weight. Additionally, the fabrication of waveguide components tends to be more expensive than planar transmission lines. As a result, most microwave filters today are designed using planar transmission lines (microstrip lines), which provide a more compact, lightweight, and cost-effective solution for modern, mobile-focused communication systems [3, 4]. Bandpass filters (BPFs) are crucial in both transmitters and receivers, playing a key role in minimizing interference. High-performance BPFs with sharp selectivity and wide stopbands are essential to meet anti-interference requirements. However, the increasingly limited and crowded spectrum presents significant challenges for designing such filters in modern wireless systems. Traditionally, enhancing BPF selectivity involves increasing the filter order, which leads to higher insertion loss.

In contrast, a quasi-elliptic response achieves comparable selectivity with fewer orders, resulting in lower insertion loss and better performance [5]. A microstrip lowpass filter with improved characteristics has been developed, incorporating a novel patch resonator with strong slow-wave effects. This arrangement allows for either a higher roll-off or a better stopband. A prototype filter was designed, fabricated, and tested, showing a 3 dB cutoff frequency of 2.4 GHz. These results showed a roll-off rate of 92.5 dB/GHz and a fractional stopband bandwidth of 135.5% measured at 30 dB of attenuation. Simulations against measurements were also performed to validate the filter's performance [6].

It realizes the compact BPFs with newly designed triple rectangular splits and further optimizes the narrowband performance at the central frequency of 3.682 GHz. An open-loop twin rectangular resonator is utilized in the proposed configuration for both Tx and Rx filters. This allows the filter to realize the prominent roll-off rate of 87 with a bounded transition band of 0.196 GHz. These results show excellent scattering characteristics, including a return loss of 27.48 dB with an insertion loss of only 0.38 dB for S21, while showing remarkable compactness with a size of 24 mm×24 mm. Using split rectangular resonators has significantly enhanced the performance and drastically reduced the filter's dimensions. Other noticeable features are the exact control of resonances and negligible signal degradation, which will act as pointers toward the potential of this design in advanced communication systems. The filter design presented here outperforms those reported so far while setting a base for further development toward high-performance filtering technologies.

2. Related works

As wireless communication technology advances, the design process related to filters, duplexers, and triplexers has also significantly improved. The following sections focus on some significant research related to the current work. In [7], a new LPF featuring a compact configuration and broad bandwidth rejection is implemented using TRSs. The operational principle is developed through an equivalent-circuit model, and the fabricated LPF features a cutoff frequency equal to 3 GHz with a maximum stopband rejection up to 24 GHz (8fc). The selectivity in the skirt, due to the generation of multiple zeros made possible by the presence of TRSs, is 144 dB/octave, while the insertion loss within the passband is lower than 1.5 dB. Input/output loading cells have also been used to extend the stopband performance further, well beyond 40 GHz (13fc).

In [8], design an LPF with a sharp cutoff response and a wide rejection bandwidth. The design combines semi-circle stepped-impedance stubs, semi-circle defected ground structures, and microstrip coupled-line hairpin units. Simulations and measurements reveal consistent results, confirming the effectiveness of the design. In [9], an LPF using a stepped-impedance hairpin resonator is presented, where radial stubs are added to achieve broad stopband rejection. The filter occupies only $0.08\lambda g \times 0.08\lambda g$ and demonstrates strong agreement between measured and simulated performance. In [10], a lowpass filter (LPF) with a simple structure is proposed, consisting of a microstrip coupled-line hairpin unit, a spiral slot, and two open stubs. The filter is designed with a 3 dB cutoff frequency of 2.0 GHz, demonstrating excellent agreement between theoretical, simulated, and measured results.

The paper [11] presents the development of a microstrip LPF featuring curved stepped-impedance resonators and T-shaped with folded lines. For this filter, the cutoff frequency is optimum at 1.5 GHz. The obtained transition band is from 1.5 GHz to 1.71 GHz, corresponding to an attenuation of -3 dB and -20 dB, respectively. It features at least 20 dB stopband attenuation from 1.71 to 20 GHz, with less than 0.1 dB insertion loss, for a compact area of 0.017 λg^2, corresponding to 28 × 13 mm^2. The agreement can be observed between simulated and measured results. Another wide stopband lowpass filter has been presented in [12]. A resonator was realized using two nested stepped-impedance hairpin units. This structure introduces additional transmission zeros that allow a sharp transition and a wide stopband. A prototype under 1.6 GHz can be implemented in compact dimensions of 0.081λg × 0.113λg that provides a stopband rejection of 20 dB up to 15 GHz. In [13], a compact and highly selective LPF featuring a wide stopband is implemented using coupled rhombic stubs. The filter unit is realized by introducing a rhombic stub in the transmission line, while the folded three-element configuration provides compactness and selectivity due to the coupling between stubs. The final design shows the extended stopband up to 11.5fc and better rejection than 35 dB. The designed filter has a compact dimension of 0.12λg × 0.10λg and achieves an excellent FOM of 27,142.

3. Methodology

This paper presents a new design method of microstrip BPF using open-loop resonators. Having different characteristics coupled to input and output terminals are designed in such a way that input terminals allow the transfer of energy not only through electric but also magnetic coupling mechanism; the design is based on a new substrate that applies our design that has good characteristics, especially in loss tangent=0.001 with dielectric constant equal 3 and thickness=1.52mm otherwise AWR program is used to simulate the proposed BPF.

3.1. Microstrip resonators

A resonator is an electromagnetic element demonstrating a resonant characteristic in many frequency applications, such as filters, frequency meters, oscillators, and phase equalizers. Resonators are classified into two categories: lumped capacitances and inductances. Lumped elements must be significantly smaller than a wavelength, which means they are less effective at microwave frequencies where the wavelength is relatively short. The other one is the distributed transmission line resonator with similar characteristics to lumped element resonators, which is applicable for microwave frequencies [14]. The distributed single resonator circuits have a transmission line resonator structure and a coupling gap between the resonator and feed lines. The characteristic behavior depends on its physical dimensions and substrate materials [15].

The quality factor, or Q-factor, is a crucial parameter used to describe the performance of resonators, including microstrip resonators. The quality factor measures the energy stored in the resonator relative to the energy lost per cycle. It provides insight into the resonator's efficiency and ability to maintain oscillations at a particular frequency. The quality factor (Q) is the inverse of the fractional bandwidth of the resonator. The bandwidth (Δf) is measured at the half-power points, as illustrated in Figure 1. (Δf) is also known as the two-sided -3 dB bandwidth [16].

$$Q = \frac{f_0}{\Delta f} \ldots\ldots (1)$$

where f_0 is the center frequency, Δf is the bandwidth, and Q is the quality factor

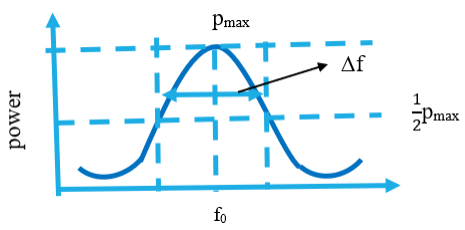

Figure 1. Transfer characteristic of the resonant circuit

Depending on its connection or loading, there are various quality factors for a microstrip line. The unloaded quality factor (Qu) refers to the quality factor of the line when it is not connected to any external circuit. The loaded quality factor (QL) is the quality factor of the line when connected to a load impedance. When coupled to another line or circuit, the external quality factor (Qe) is the line's quality factor. The following formula relates these quality factors [16, 17].

Many types of resonators are used to design filters, diplexers, and triplexers. The most important of them include lumped-element resonators, which use discrete components like capacitors, inductors, and sometimes resistors, which are treated as ideal, frequency-independent components. These elements are typically used in low-frequency circuits, where the physical dimensions of the components are much smaller than the wavelength of the operating frequency. At the same time, quasi-lumped-element resonators mimic the behavior of lumped elements but are realized using distributed elements such as short sections of transmission lines. Quasi-lumped elements are engineered to mimic the behavior of lumped components at specific frequencies.

Another type of resonator used in microstrip applications is the distributed resonator, which is widely used in microwave engineering. These resonators achieve their resonant behavior through the distributed electromagnetic fields along a microstrip transmission line. They typically resonate at lengths of $\lambda g/4$ and $\lambda g/2$, where λg is the guided wavelength at the fundamental resonant frequency, $f0$. This resonator type is also called a uniform impedance resonator (UIR). Stepped impedance resonators (SIRs) represent another category of microstrip resonators. These distributed resonators consist of alternating transmission line sections with varying characteristic impedances. The impedance "steps" between high and low values along the length of the SIR enable precise control of the resonant frequencies and support compact designs. SIR resonators are known for their high quality (Q) factor and efficient energy storage, making them ideal for use in bandpass filters. Figure 2 illustrates a typical microstrip.

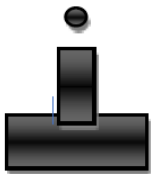

Figure 2. Microstrip quasi-lumped-element resonator

The conventional half-wavelength resonator, depicted in Figure 3 (c), can be adapted into various folded shapes. Standard configurations derived from the microstrip half-wavelength resonator include the hairpin, square open-loop, and rectangular resonators, as illustrated in Figures 3(d) and (e). The stepped-impedance resonator (SIR) exhibits discrete changes in impedance, resulting in a broader bandwidth compared to uniform impedance resonators (UIR), diplexers, and impedance transformers, as shown in Figure 3(f) [16][1][18].

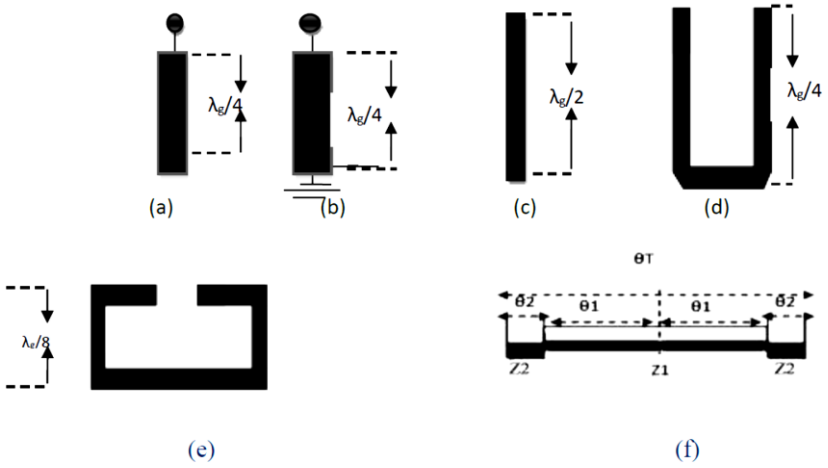

Figure 3. Presents different resonator configurations, including (a) a quarter-wavelength resonator for shunt-series resonance, (b) a quarter-wavelength resonator for shunt-parallel resonance, (c) a half-wavelength resonator, (d) a hairpin resonator, (e) a square open-loop resonator, and (f) a stepped-impedance resonator (SIR) [1]

Filters are vital components in RF and microwave systems, separating or combining various frequencies. Given the finite and shared nature of the electromagnetic spectrum, filters are essential for restricting RF/microwave signals to their allocated spectral ranges. With advancements in applications like wireless communications, RF/microwave filters face increasing demands for enhanced performance, reduced size, lighter weight, and lower cost. These filters are classified as active or passive based on specific requirements and design criteria [1]. Active filters integrate active components, including transistors, diodes, and amplifiers, alongside traditional passive elements. These filters are relatively straightforward to implement, offer gain, and can achieve a high-quality factor. Additionally, they integrate seamlessly with other system components. However, the presence of active elements means that these filters require an external power supply, which can increase the overall system complexity [2].

There are four types of filters classified according to the frequency response as follows:

Lowpass filters are commonly utilized to allow signals or currents below a specified frequency to pass while attenuating those above this threshold. These filters are particularly effective for emission control, as problematic signals often manifest as harmonics far above their fundamental frequency. Figure 4 illustrates the characteristic response of a lowpass filter, where f represents the frequency and fc denotes the cutoff frequency [19].

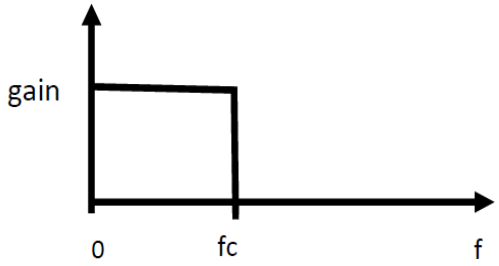

Figure 4. Characteristics of the low-pass filter

The high-pass filter is the opposite of a low-pass filter. It has a high impedance below the cutoff frequency, allowing signals above it to pass. High-pass filters are often used to eliminate power line noise from signal lines. They are commonly employed for electromagnetic interference (EMI) reduction. Combined with a lowpass filter (LPF), it can form a bandpass filter [19]. The characteristic response of the high-pass filter (HPF) is illustrated in Figure 5.

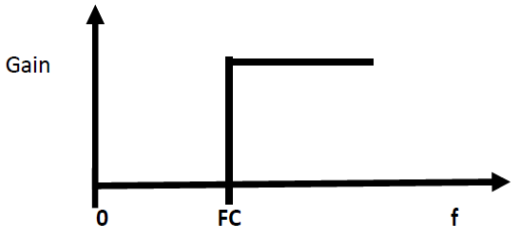

Figure 5. The high-pass filter characteristic

Bandpass filters are designed to exhibit low impedance within a specific frequency range, defined by an upper boundary (fH) and lower boundary (fL), while maintaining significantly higher impedance outside this range. These filters attenuate and reject signal components outside the fL and fH bands. They are frequently employed in systems utilizing frequency-division multiplexing, such as voice-frequency telegraph terminals, to manage individual channels. In cellular radio base station transmitters and receivers, bandpass filters are critical components of the radio frequency (RF) front end. The transmitter's primary function is to confine the output signal's bandwidth to the allocated transmission band, thereby preventing interference with other stations. In receivers, bandpass filters enable the reception and decoding of signals within the desired frequency range while blocking unwanted frequencies, as illustrated in the figure below [1][19].

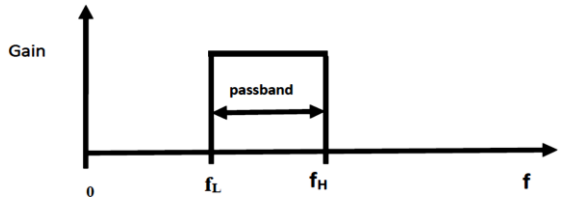

Figure 6. Bandpass filter characteristic

A band-stop filter (BSF), also called a band-reject filter, is the inverse of a bandpass filter. It rejects or attenuates signals within a specific frequency band while allowing all other signals outside it to pass. For example, a BSF with lower and upper-frequency boundaries (fL and fH) will block the signal components between fL and fH, termed the stopband, while transmitting all other frequencies [1], as shown in Figure 7.

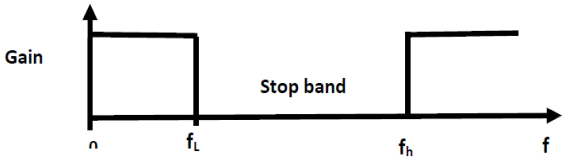

Figure 7. Band-stop filter characteristic

4. Specifications of microwave filters

Return loss, or reflection loss, represents the fraction of power not successfully delivered from a source to a load. It is measured in decibels and calculated using the incident power (Pi) and the reflected power (Pr). A well-matched load reduces reflected power, resulting in a higher return loss. This metric is positive when the reflected power is less than the incident power [20, 21].

$$RL = 10 \log_{10} (P_i/P_r)\ dB……..(2)$$

P_r=reflected power

P_i=input power

Insertion loss is the amount of power lost when a signal is transmitted through a transmission line. In the case of microstrip transmission lines, insertion loss is a combination of conductor loss, dielectric loss, and radiation loss. Calculating the insertion loss of a microstrip line requires knowledge of the line's geometry, dielectric properties, and frequency. The conductor loss is a function of the line's resistance per meter and characteristic impedance. Dielectric loss depends on the dielectric constant and the loss tangent of the substrate material, while radiation loss is influenced by the length of the line and the signal frequency [22].

$$IL=10\log_{10}(P_i/P_t)…….(3)$$

P_i=incident power

P_t=transmitted power

A passband refers to the range of frequencies or wavelengths a filter allows to pass through, whereas a stopband is a range of frequencies defined within specific limits that the filter blocks or attenuates.

The cutoff frequency is when the filter's insertion loss reaches 3 dB. This point commonly indicates the boundary between the passband and the stopband.

Gap coupling is an important parameter to consider when designing microwave filters. There are two primary types of gap coupling: a gap between the feed lines and the resonator and a gap between resonators. The high value of an unloaded quality factor is preferable when designing microstrip filters. This is usually done by either a direct connection coupling or couplings by a small gap to ensure that the loaded Q remains high; gap coupling can be between a feed line and resonators or two resonators; the basic circuit comprises feed lines, coupling

gaps, and a resonator. One possible arrangement is illustrated in Figure 8, which utilizes an open-loop resonator as an example.

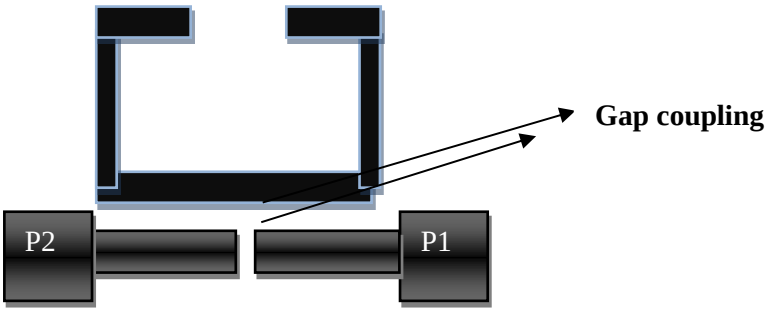

Figure 8. Gap coupling

The feed lines transfer power into and out of the resonator. They are positioned at a specific distance from the resonator, known as the coupling gap. This gap must be carefully sized: it should be large enough to minimize any significant disturbance to the fields within the resonator, yet minor enough to ensure adequate power coupling. The appropriate coupling is crucial for optimizing the circuit for its intended application [23, 24].

5. The filter design and results

The bandpass filter (BPF) structure is introduced in the initial step of the design process. These BPFs are designed using triple rectangular loop resonators, which can be arranged to create a microstrip quad-channel diplexer for applications in 5G and WLAN. Firstly, triple rectangular loop resonators are combined where electric and magnetic coupling between the combined resonator; otherwise, external coupling takes place also with two ports having SIR, the internal resonators that consist of several UIR resonators that must be thin, not thick UIR, BPF is shown in Figure 9.

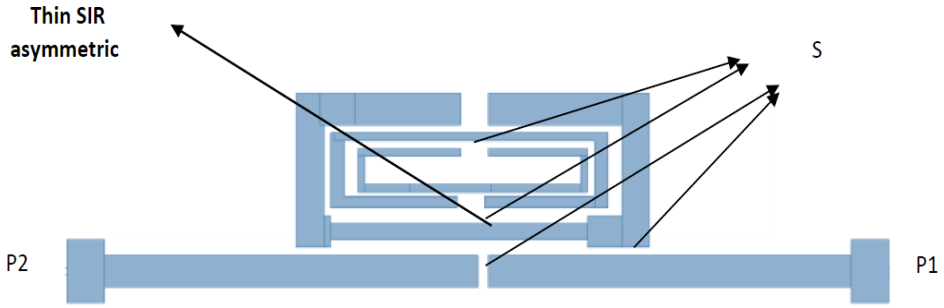

Figure 9. Triple open-loop rectangular BPF

The proposed filter is numerically investigated using the AWR office. The scattering coefficients of the filter are shown in Figures 10 and 11, and S12 is shown in Figure 10. It can be seen that a good matching condition is obtained at 0.3851 dB. Also, the transmission coefficient S11 is shown in Figure 11 with a center frequency of 3.682 GHz.

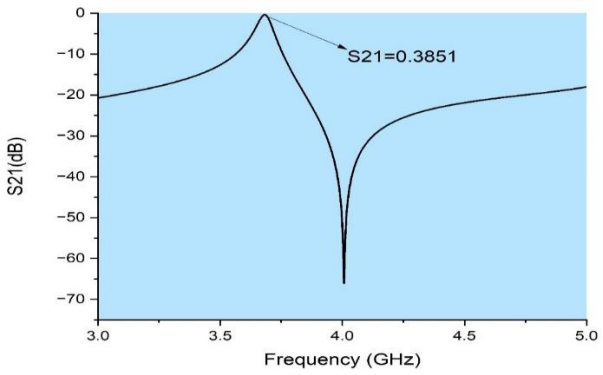

Figure 10.S21 response

In the proposed bandpass filter (BPF) design, several gaps create coupling, which can be either electric or magnetic. Both types of coupling occur in the design, and these gaps, denoted as "S," play a crucial role. Adjusting the value of S allows for tuning the frequency and the S-parameters of S11 and S21. The most significant space between the two feed lines and the external resonator can significantly affect the values of the S-parameters. The optimal performance, characterized by the lowest insertion loss and most significant return loss, occurs when S=0.2 mm S=0.2mm. The use of triple small rectangular resonators yields promising results. However, if one of these resonators is removed and only two resonators are used, the final performance deteriorates, with S11=−11.1dB and an insertion loss of 0.82 dB. The proposed BPF achieves a transmission zero (TZ) at 4.007 GHz, which provides a stopband near this frequency. The bandwidth (BW) is 61 MHz, with a fractional bandwidth (FBW) of 1.7%.

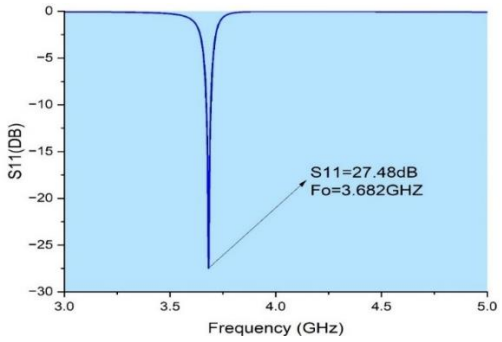

Figure 11.S11 response for lower BPF

Three cases changed to see effects on this filter if used thick asymmetric SIR that considers external resonators will give S11=21.44 dB, S21=0.388 dB while the mismatch of impedance reduces to 1.185 at 3.886 GHz, the second cases that used symmetric external SIR direct coupling with two external ports given S11=12.06 dB, S21=0.6 dB at 3.701GHz, third cases used UIR instead of SIR at two ports making the performance degraded to be given S11=17dB, S21=0.44dB at 3.96 GHz.

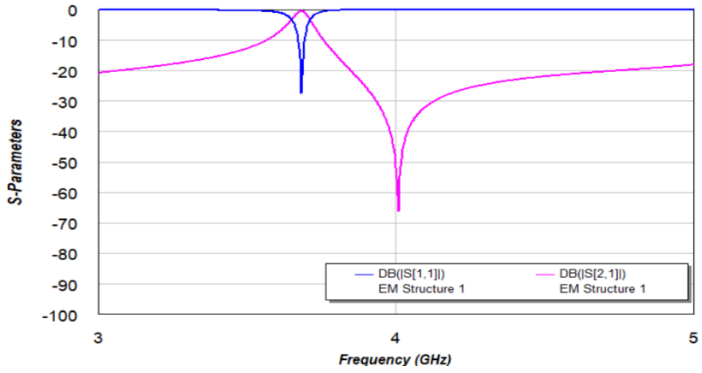

Figure 12. S-parameters for BPF

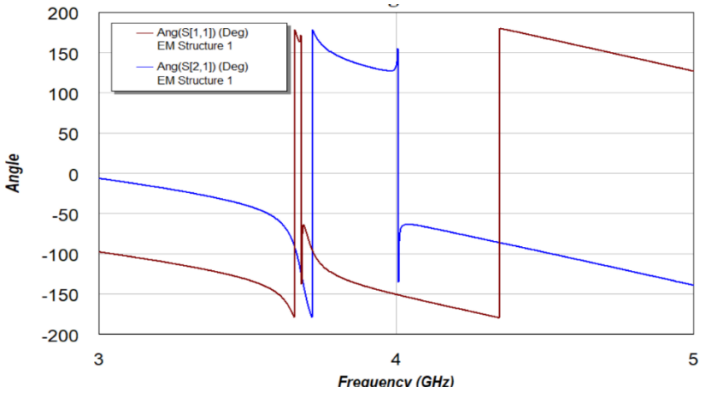

Figure 13. Phase response for BPF

The graph in Figure 13 shows the phase angle characteristics of the bandpass filter (BPF) across a frequency range of 3 GHz to 5 GHz; near the filter's central frequency (3.682 GHz), there is a sharp change in phase for both S11 and S21. This rapid phase transition is characteristic of resonant behavior, where the filter's performance is optimized for minimal reflection and maximal transmission [25]. The steep phase transitions around the passband highlight the filter's sharp selectivity and suitability for applications requiring precise frequency isolation.

Figure 14 represents the group delay characteristics of the bandpass filter (BPF) across a frequency range of 3 GHz to 5 GHz. Group delay is a critical metric that indicates the time delay of a signal passing through the filter at a specific frequency. This group delay plot confirms the excellent performance of the BPF, with sharp transitions near the resonance and stable behavior elsewhere. The observed characteristics make the filter suitable for high-precision applications requiring both selectivity and timing accuracy.

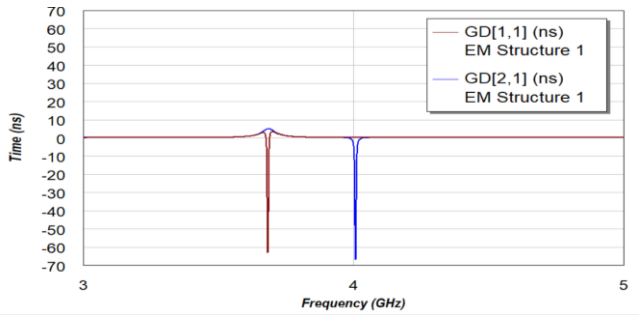

Figure 14. Group delay for BPF

In Figure 15, the plotted VSWR values across the operational frequency bands illustrate how effectively the triplexer maintains impedance matching. Ideally, the VSWR should remain close to 1:1 across the desired frequencies to ensure optimal performance. Higher values at specific frequencies suggest areas where adjustments are needed, such as modifying the load's impedance or using matching networks to improve efficiency. Understanding and minimizing VSWR is essential for ensuring that the RF transmitter operates effectively, reducing the risk of damage due to reflected power and improving overall system performance. Proper design and calibration can achieve a lower VSWR, thereby enhancing the reliability and effectiveness of the communication system. The VSWR can be calculated using the reflection coefficient based on:

$$VSWR=1-|\Gamma|/1+|\Gamma|\ldots\ldots\ldots(4)$$

$$\Gamma=ZL+Z0/ZL-Z0\ldots\ldots\ldots(5)$$

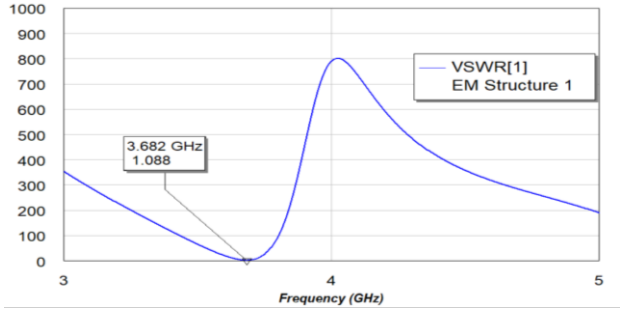

Figure 15.VSWR for BPF based on S11 parameter

The following steps explain the results shown in Figure 15:

1. VSWR close to 1: A VSWR close to 1 represents an ideal impedance match with minimal reflected power, leading to efficient signal transmission [26].

2. High VSWR (e.g., >10): High VSWR values indicate a significant impedance mismatch, resulting in poor performance and high reflected power [27].

3. Intermediate VSWR (2-4): An intermediate VSWR value suggests a moderate mismatch, which may be acceptable depending on the application but could still lead to signal degradation [28].

The guided wavelength, indicated by λg, is calculated by using:

$$\lambda g = \frac{c}{fo\sqrt{\epsilon eff}} \quad \ldots\ldots..(6)$$

In this particular equation, 'c' represents the speed of light, while 'f_o' denotes the center frequency. The symbol 'єeff' means the effective dielectric constant of the specific material used. In this case, the guided wavelength in this filter is determined to be approximately 0.0549 meters. Based on the characteristics of the waveguide, it is reasonable to propose a diplexer size of 0.437λg × 0.437λg. This design will significantly complement the guided wavelength.

The roll-off rate refers to the rate at which the filter's attenuation increases as a function of frequency after the cutoff point

$$Ɛ=\frac{\alpha max-\alpha min}{fs-fc}\ldots\ldots.(7)$$

αmax *and* αmin are -20 and -3 dB attenuation points, respectively. Fc is the -3 dB cutoff frequency, and fs is the -20 dB stopband frequency [11, 29, 30].

The suppression factor (SF) is based on the rejection level in the stopband bandwidth. For example, when there is a 20dB suppression, the corresponding SF is 2. A higher suppression means a greater SF.

SF=Rejected level in the stopband/10……....(8) [11, 29, 30].

The normalized circuit size (NCS) is a metric used to describe the size of a filter or resonator in terms of a normalized or standardized measure, often relative to some characteristic dimension such as wavelength, frequency, or design parameters. It is commonly used in RF (radio frequency) and microwave filter design to assess a filter or resonator's physical or electrical dimensions compared to its operating frequency or a reference dimension**.** Smaller NCS values indicate smaller filter or circuit sizes relative to the operating wavelength.

NCS=Physical size (length×width)/ λ^2_0 ……..(9) [11]

λ^2_0: The wavelength corresponds to the operating frequency f_0 (usually the resonant or cutoff frequency).

Where the architecture factor (AF) for a planar is defined as 1 and 2, respectively, if the design is complex =2; otherwise =1.

Table 1 compares the BPF developed in this work with those described in references [7-13]. The proposed microstrip BPF significantly outperforms its contemporaries regarding compactness and insertion loss (IL) performance. Additionally, key aspects such as insertion loss, return loss, roll of rate, and NCS are detailed in this table. Narrowband bandpass filters can enhance security and reliability for communication systems using isolating desired signals, refining detection capabilities, and mitigating various types of cyber threats. Their integration into cybersecurity measures can lead to more robust and secure network infrastructures [31, 32]

Table 1. Comparing BPF in this article with the other reported studies.

Ref	Ɛ	Return loss(dB)	Insertion loss(dB)	NCS
[7]	62	10		0.31×0.24
[8]	42.5	12	1.5	0.101×0.24
[9]	30	12	0.5	0.08×0.08
[10]	43.9	-----	1	0.101×0.15
[11]	81	20	0.1	0.14×0.065
[12]	52.8	20	0.3	0.081×0.113
[13]	57.8	11	2	0.12×0.1
The proposed filter	87	27.48	0.38	0.12×0.12

6. Conclusion

The designed bandpass filter, optimized at 3.682 GHz, offers good performance with a low insertion loss of 0.38 dB, high selectivity, and superior impedance matching. Its compact size and sharp roll-off make it ideal for space-constrained modern communication systems.

Declaration of competing interest

The authors declare that they have no known financial or non-financial competing interests in any material discussed in this paper.

Funding information

The authors declare that they have received no funding from any financial organization to conduct this research.

Author contribution

Aqeel H. Al-Fatlawi: Conceptualization of the study, design of the microstrip bandpass filter, and writing of the original draft.

Sadra Kashef: Conducted simulations and analysis of the filter performance, contributed to the methodology, and assisted in manuscript preparation.

Yaqeen Sabah Mezaal: Provided insights into the design process, performed experimental validation, and contributed to the discussion of results.

Morteza Valizadeh: Supervised the project, provided critical revisions to the manuscript, and ensured the integrity of the research.

References

[1] Y. S. Mezaal, H. T. Eyyuboglu, and J. K. Ali, “A new design of dual band microstrip bandpass filter based on Peano fractal geometry: Design and simulation results,” in 2013 13th Mediterranean Microwave Symposium (MMS), 2013.

[2] Y. S. Mezaal and H. T. Eyyuboglu, “A new narrow band dual-mode microstrip slotted patch bandpass filter design based on fractal geometry,” in *2012 7th International Conference on Computing and Convergence Technology (ICCCT)*, 2012, pp. 1180–1184.

[3] 3-A. Balalem, Analysis, design, optimization, and realization of compact high-performance printed RF filters, Ph.D. dissertation, Magdeburg Univ., Magdeburg, Germany, 2010.

[4] M. A. Alqaisy, “Dual-Band Pass Filter with Wide Band-Frequency Rejection”, AL-IRAQIA JOURNAL FOR SCIENTIFIC ENGINEERING RESEARCH, no. 00, pp. 1–5, Mar. 2022.

[5] Y. S. Mezaal, H. T. Eyyuboğlu, and J. K. Ali, “New microstrip bandpass filter designs based on stepped impedance Hilbert fractal resonators,” IETE J. Res., vol. 60, no. 3, pp. 257–264, 2014.

[6] J. L. Li, S. W. Qu, and Q. Xue, "Compact microstrip lowpass filter with sharp roll-off and wide stopband," Electronics Lett., vol. 45, no. 2, pp. 110-111, 2009.

[7] K. Ma and K. S. Yeo, "New ultra-wide stopband lowpass filter using transformed radial stubs," IEEE Trans. Microwave Theory Tech., vol. 59, no. 3, pp. 604-611, Mar. 2010.

[8] F. Wei, L. Chen, X. W. Shi, Q. L. Huang, and X. H. Wang, "Compact lowpass filter with wide stopband using coupled-line hairpin unit," Electronics Lett., vol. 46, no. 1, pp. 1, Jan. 2011.

[9] X. B. Wei, P. Wang, M. Q. Liu, and Y. Shi, “Compact wide-stopband lowpass filter using stepped impedance hairpin resonator with radial stubs,” Electronics Lett., vol. 47, no. 15, pp. 1, Jul. 2011.

[10] F. Wei, L. Chen, and X. W. Shi, “Compact lowpass filter based on coupled-line hairpin unit,” Electronics Lett., vol. 48, no. 7, pp. 1, Apr. 2012.

[11] M. Hayati, H. Abbasi, and F. Shama, “Microstrip lowpass filter with ultrawide stopband and sharp roll-off,” Arabian J. Sci. Eng., vol. 39, pp. 6249-6253, 2014.
[12] S. Liu, J. Xu, and Z. Xu, “Compact lowpass filter with wide stopband using stepped impedance hairpin units,” Electronics Lett., vol. 51, no. 1, pp. 67-69, 2015.
[13] B. Zhang, S. Li, and J. Huang, “Compact lowpass filter with wide stopband using coupled rhombic stubs,” Electronics Lett., vol. 51, no. 3, pp. 264-266, 2015.
[14] R. S. Elliott, An Introduction to Guided Waves and Microwave Circuits, 2nd ed. New Jersey: Prentice-Hall, 1993.
[15] T. J. Bryant and A. Weiss, "Parameters of microstrip transmission lines and coupled pairs of transmission lines," IEEE Trans. Microwave Theory Tech., vol. 16, no. 12, pp. 1021-1027, Dec. 1968.
[16] D. M. Pozar, Microwave Engineering, 4th ed. John Wiley & Sons, 2011.
[17] T. C. Edwards and M. B. Steer, Foundations for Microstrip Circuit Design, 4th ed. John Wiley & Sons, 2016.
[18] I. Wolff and R. D. Knoppink, “Microstrip bandpass filter using parallel-coupled lines,” Electronics Lett., vol. 7, no. 26, pp. 779-781, Dec. 1971.
[19] B. C. Gabrielson, Basic Active and Passive Filters.
[20] Standard Reference Data Database, U.S. National Institute of Standards and Technology and References.
[21] International Council for Science: Committee on Data for Science and Technology.
[22] “Insertion loss of microstrip line of RO4350B PCB at 24GHz,” [Online]. Available: http://ipcb.com.
[23] Y. Sun, L. Xu, C. Peng, and Z. Li, “Incident light influence on the transmission of coupled ring resonators,” Tsinghua Sci. Technol., vol. 15, no. 2, pp. 198-201, 2010.
[24] K. Chang, Microwave Ring Circuits and Antennas.
[25] A. H. Al-Fatlawi and M. A. Taha, “New microstrip filter for MIMO wireless and computer systems,” J. Theoretical & Appl. Information Tech., vol. 96, no. 12, 2018.
[26] T. F. Skaik, M. J. Lancaster, and F. Huang, “Synthesis of multiple output coupled resonator circuits using coupling matrix optimization,” IET Microwaves, Antennas & Propagation, vol. 5, no. 9, pp. 1081-1088, 2011.
[27] A. Rezaei, L. Noori, and H. Mohammadi, “Design of a miniaturized microstrip diplexer using coupled lines and spiral structures for wireless and WiMAX applications,” Analog Integrated Circuits and Signal Processing, vol. 98, pp. 409-415, 2018.
[28] C. Perez-Wences, J. R. Loo-Yau, I. Lavandera-Hernandez, P. Moreno, A. J. Reynoso-Hernandez, and L. M. Aguilar-Lobo, “Compact microstrip lowpass-bandpass diplexer using radial stubs,” Microwave and Optical Technology Lett., vol. 61, no. 2, pp. 485-489, 2019.
[29] F. Yousefi Moghadam, B. Afzali, F. Nadi, and R. Zallbeygi, “Compact low pass filter using sharp roll-off ultra-wide stopband T-shaped resonator,” Journal of Electrical and Computer Engineering Innovations (JECEI), vol. 6, no. 1, pp. 25-31, 2017.
[30] V. K. Velidi and S. Sanyal, “Sharp roll-off lowpass filter with wide stopband using stub-loaded coupled-line hairpin unit,” IEEE Microwave and Wireless Components Letters, vol. 21, no. 6, pp. 301-303, Jun. 2011.
[31] S. A. AbdulAmeer *et al.*, "Cyber Security Readiness in Iraq: Role of the Human Rights Activists," *International Journal of Cyber Criminology*, vol. 16, no. 2, pp. 1–14-1–14, 2022.
[32] Y. Sh. Ajaj, B. R. Al-Kaseem, and Y. Al-Dunainawi, “Cyber Attacks in SDN-Based IoT Environment: A Review”, *Al-Iraqia Journal for Scientific Engineering Research*, vol. 2, no. 3, pp. 74–83, Sep. 2023.